Length-Controlled Rodlike Self-Assemblies in Binary Mixed Langmuir−Blodgett Monolayers on Mica

Hongbo Li, Qingtao Liu, Miao Xu, Weifeng Bu, Xiankun Lin, Lixin Wu,* and Jiacong Shen

Key Laboratory for Supramolecular Structure and Materials of Ministry of Education, Jilin University, Changchun, 130012, PRC

Received: July 19, 2004; In Final Form: November 23, 2004

In this paper, atomic force microscopy (AFM) has been used to investigate the morphology of monolayers of the amphiphilic rod−coil diblock molecule (EO_7OPV) containing oligo(phenylene vinylene) dimer (OPV) and poly(ethylene oxide) (PEO) as well as the morphology of mixed monolayers of EO_7OPV and palmitic acid (PA) deposited onto mica by the Langmuir−Blodgett technique. At surface pressures higher than 3 mN/m, EO_7OPV forms regular-shaped aggregates with a monomolecular layer structure, where the hydrophilic PEO blocks are adsorbed onto the mica substrate and the hydrophobic OPV blocks form an ordered crystalline OPV layer on the top of the PEO layer through the strong $\pi-\pi$ stacking interaction. In the mixed LB monolayers of EO_7OPV and PA, the phase separation occurs. At a certain mixed ratio, EO_7OPV molecules form rodlike domains with regular shape and uniform size at surface pressures higher than 3 mN/m. With the increase of the molar fraction of PA, the rodlike domains consisting of EO_7OPV are elongated. The length of the rodlike domains can be tuned easily in a large range by altering the molar ratio of EO_7OPV and PA. In addition, the rodlike domains are oriented to specific directions, corresponding to the directions of the potassium ion array on the mica surface having 6-fold symmetry. We demonstrate the possible formation mechanism and the elongation origin of rodlike domains in mixed LB monolayers and propose the two-step formation process of oriented rodlike domains deposited onto the mica substrate.

Introduction

The fabrication of self-assembly architectures with well-defined structures is a long-standing and important topic in surface and material science.[1−4] Rod−coil molecules as a typical self-assembly system have been widely investigated in the solution and solid state, where they are capable of self-assembling into various nanostructures such as lamellar, cylindrical, spherical, and other structures.[5−7] The investigations concerning thin-film structures of rod−coil molecules at solid supports are rarely found.[8] As a matter of fact, understanding and controlling their nanostructures on solid surfaces are essential for their function and application. A general approach to various nanostructural designs of rod−coil molecules is focused on the modifications of their chemical structure, molecular composition, and molecular weight, which usually needs a complex synthesis process.[9,10] Nevertheless, to fabricate self-assembly nanostructures with controlled sizes and shapes by an easier way is still a great challenge in this field.

Two-dimensional self-assembly patterns can be fabricated by utilizing the phase separation of multicomponents or the different phase coexistence of single components in Langmuir−Blodgett (LB) monolayers.[11−21] The nanosized domains with circular, spiral, needlelike, and stripelike shapes have been observed in the phospholipid or mixed fatty acid Langmuir monolayers or LB monolayers.[16−21] The domain shapes in equilibrium are thought to be controlled by the two competing effects at the air−water interface: the line tension between two-phase boundaries and the long-range electric dipolar interactions between molecules.[22,23] Therefore, the shape and size of self-assemblies consisting of amphiphilic rod−coil molecules may be controlled by simply tuning the two competing effects at the air−water interface.

In the previous work, we have synthesized amphiphilic rod−coil diblock oligomers containing the hydrophobic oligo(phenylene vinylene) (OPV) dimer as the rod segment and the hydrophilic poly(ethylene oxide) (PEO) as the coil segment.[24−26] Through controlling atmosphere humidity at the solid−air interface, we fabricated two different self-assembly nanostructures on mica: nano island with a monolayer structure formed under the dry atmosphere and nano ribbon with a bilayer structure formed under the humid atmosphere.[25,26] Herein, we have obtained regular-shaped rodlike domains consisting of an amphiphilic rod−coil diblock oligomer (EO_7OPV, Scheme 1) in the mixed LB monolayers of EO_7OPV and palmitic acid (PA) on mica. Significantly, the length of these rodlike domains can be tuned easily by altering the molar ratios between EO_7OPV and PA. We demonstrated the possible formation mechanism and the elongation origin of rodlike domains in mixed LB monolayers and proposed the two-step formation process of oriented rodlike domains on mica. The monolayer behaviors at the air−water interface were studied by pressure−area ($\pi-A$) isotherm measurements. The surface structures and morphologies in the LB monolayers of EO_7OPV and mixed LB monolayers of EO_7OPV and PA were observed using the AFM technique.

Experimental Section

Synthesis of a rod−coil molecule was similar to our previous work[25] and it was characterized with NMR, IR, and MALDI-TOF mass spectrum. The PEO block comes from commercially

* Corresponding author. Tel: +86-431-5168481. Fax: +86-431-5193421. E-mail: wulx@jlu.edu.cn.

10.1021/jp046816u CCC: $30.25
Published on Web 01/20/2005

SCHEME 1: Chemical Formula of EO_7OPV

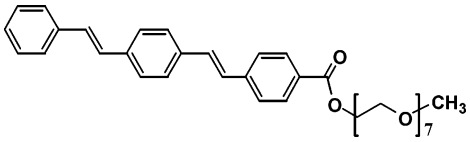

available poly(ethylene glycol) with an average molecular weight of 350. The chemical structure of the rod−coil molecule and the number of repeating units in the PEO coil were confirmed by ^{1}H NMR spectrum. The rod−coil molecule has a molecular weight distribution with polydispersity index of 1.06, indicative of high purity. ^{1}H NMR (500 MHz, $CDCl_3$): 8.05 (d, 2H, $J = 8$ Hz), 7.58 (d, 2H, $J = 8$ Hz), 7.54 (s, 4H), 7.52 (d, 2H, $J = 8$ Hz), 7.37 (t, 2H, $J = 8$ Hz), 7.26 (t, 1H, $J = 8$ Hz), 7.21−7.13 (q, 2H, $J = 15.6$ Hz), 7.18−7.12 (q, 2H, $J = 16$ Hz), 4.48 (t, 2H, $J = 4.8$ Hz), 3.85 (t, 2H, $J = 4.8$ Hz), 3.72 (t, 2H, $J = 4.8$ Hz), 3.68−3.64 (m, 20H, $J = 4.8$ Hz), 3.54 (t, 2H, $J = 4.8$ Hz), 3.37 (s, 3H). IR (KBr, cm^{-1}): 3052, 3080 cm^{-1}, aromatic CH stretching; 3021 cm^{-1}, trans C═C double bond CH stretching; 962 cm^{-1}, trans C═C double bond CH wagging; 2870, 2917 cm^{-1}, CH_2 symmetric and anti-symmetric stretching mode; 1716 cm^{-1}, C═O stretching mode of aryl ester; 1602 cm^{-1}, symmetric benzenyl ring stretching; 1109 cm^{-1}, C−O−C out-of-plane bending. *m*/*z*: $(M + Na)^+$ 586.9, 631.4, 675.2, 718.9, 763.0, 808.5, 851.8, 895.4. According to ^{1}H NMR and the IR spectrum, the two double bonds in the OPV block are in the state of trans configuration. The mass spectrum presented a close match between calculated and experimental molecular weights. Palmitic ($CH_3(CH_2)_{14}COOH$) acid (PA) was purchased from Shanghai chemical company (>99% purity) and was used directly without further purification.

EO_7OPV, PA, and the mixtures of EO_7OPV and PA were spread onto the pure water subphase (pH 6−7) from a chloroform solution. The EO_7OPV concentration employed was 0.50 mg/mL, and the PA concentration was 1.00 mg/mL. The concentrations of mixtures of EO_7OPV and PA at the molar ratios of 2:1, 1:1, and 1:2 were 0.547 mg/mL, 0.585 mg/mL, and 0.647 mg/mL, respectively. A Langmuir trough equipped with a Wilhelmy balance as the surface pressure sensor was employed for $\pi-A$ isotherm measurements and the deposition of LB films. The temperature of the subphase was kept at 293 ± 1 K. After the solvent evaporated completely, the floating layer at the air−water interface was compressed at a speed of 20 cm^2/min to get the $\pi-A$ isotherm. The LB monolayers were transferred using the vertical dipping method at an up speed of 6 mm/min onto freshly cleaved mica substrates for AFM observations and onto quartz substrates for UV−vis spectroscopic measurements. All the LB films were relaxed for 30 min before the deposition (under the annealing condition).

AFM observations of the LB monolayers were carried out with commercial instruments (Digital Instrument, Nanoscope III, Dimension 3000), operating in tapping made at room temperature in air. UV−vis spectroscopic measurements were measured on a Shimadzu UV3100PC spectrometer in ambient conditions.

Results and Discussion

Monolayer Behavior of EO_7OPV. The PEO is surface active and can form a monolayer film despite being water-soluble when spread at the air−water interface. Above a critical surface density, the PEO will be compressed into the subphase.[27] When the solution of EO_7OPV is spread on an aqueous subphase, the hydrophilic PEO block should spread randomly, and the hydrophobic OPV block is tethered on the interface. Figure 1 shows a pressure−area ($\pi-A$) isotherm of EO_7OPV, in which the Langmuir film is continuous and collapses at the surface pressure of 23.1 mN/m. The molecular area at the collapse point is about 24.0 ± 0.2 Å^2, while the limiting area determined by extrapolating the condensed state to zero pressure is 35.0 ± 0.2 Å^2. The transmission electron microscope (TEM) and Cerius^2−molecular graphics model show that a herringbone packing of OPV rods with *a*, *b* lattice parameters of 7.95 and 5.15 Å, respectively, is the densest packing structure of OPV rods; thus, every OPV rod can occupy a lateral molecular area of 20.5 Å^2.[28] According to the crystal structure of PEO coils, four (7/2) helical molecules pass through a unit cell with parameters $a = 8.05$ Å, $b = 13.04$ Å, c (fiber axis) = 19.48 Å, and $\beta = 125.4°$, and the space group, $P2_1/a$-C_{2h}^5.[29] Therefore, the lateral molecular area of every PEO chain in the crystal structure can be found to be 21.4 Å^2. On the basis of the above-mentioned analysis, we believe that the EO_7OPV monolayer at the collapse point of its Langmuir isotherm is in the crystallike state, indicating the densest packing structure of the EO_7OPV monolayer. The isotherms of diblock molecules containing the large PEO block usually present a plateau at the surface pressure of 10 mN/m, which corresponds to a two-dimensional to three-dimensional (2D-to-3D) phase transition of the PEO block.[30,31] In our present case, the isotherm of EO_7OPV does not present a plateau at the surface pressure of 10 mN/m, which should be due to the much smaller PEO block. However, below the surface pressure of 3 mN/m (the molecular area: 60−40 Å^2), the low slope and the rounded shape of the isotherm imply a molecular rearrangement, corresponding to the compressed PEO block submerging from the air−water interface into the water subphase. Reversibility of the monolayer behavior at the air−water interface was tested by repeating compression−expansion cycles for the monolayer three times (Figure 1, inset). A modest hysteresis is observed for each cycle of EO_7OPV. The modest creep and short recovery time indicate that the long PEO chains expand to the original random coil conformation.

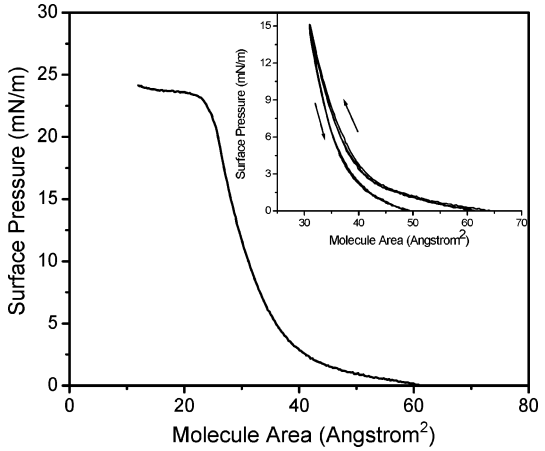

Figure 1. The pressure−area ($\pi-A$) isotherm for EO_7OPV and the hysteresis isotherm with three circles (inset section).

The LB monolayers of EO_7OPV transferred onto mica substrates at different surface pressures were studied by the AFM technique. At surface pressures of 1 mN/m and 2 mN/m, the irregular-shaped islands were observed (Figure 2A and 2B) and their transfer ratios were 0.65 and 0.62, respectively. Similar irregular-shaped domains with a much lower transfer ratio were also observed at the surface pressure of 0 mN/m. However, we observed the regular-shaped domains of EO_7OPV with a length of about 0.3−0.4 μm when the monolayers were deposited at higher surface pressures (Figure 2C, 2D, 2E, and 2F). These

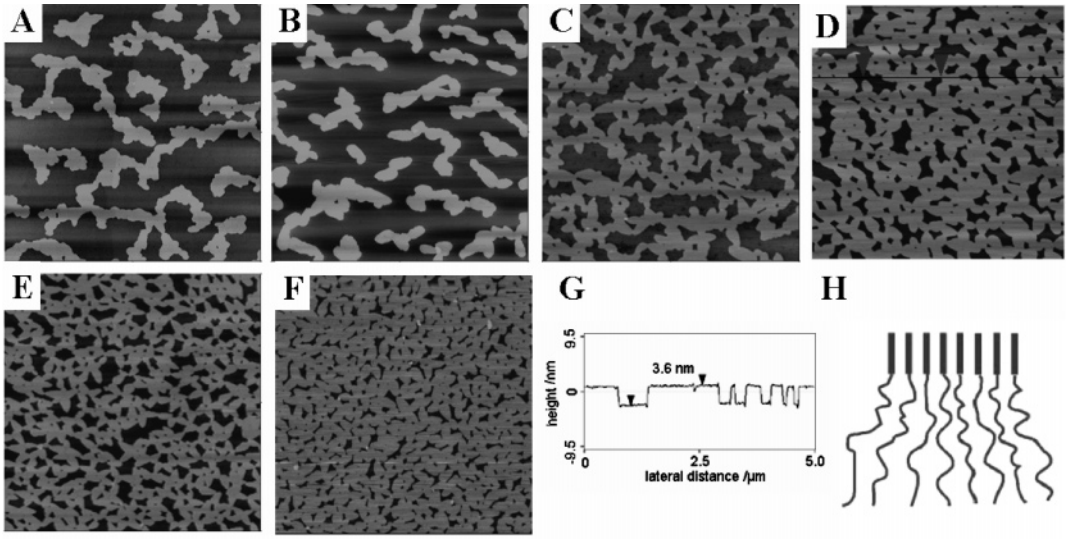

Figure 2. The height AFM images (5×5 μm) of EO_7OPV monolayers transferred onto mica at the surface pressure of (A) 1 mN/m, (B) 2 mN/m, (C) 3 mN/m, (D) 4 mN/m, (E) 6mN/m, and (F) 12 mN/m. (G) A cross section along the line indicated in (D). (H) the structural model of the monolayer LB films. *Z* range, 20 nm.

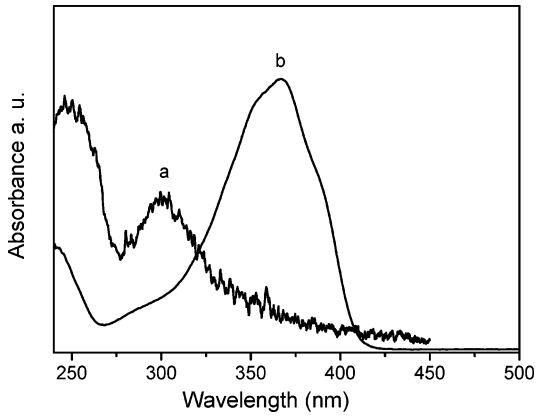

Figure 3. The UV−vis spectra of EO_7OPV: (a) the monolayer at the surface pressure of 12 mN/m; (b) the dilute solution in chloroform.

LB monolayers have larger surface coverage degrees and higher transfer ratios (near 1) compared with those deposited at the lower surface pressures. There are several proposed mechanisms concerning the formation of surface aggregates of amphiphilic block molecules deposited onto solid substrates by the LB technique. Goncalves et al. believed that the surface aggregates were a transfer of micelles in the spreading solution.[31] Thomas et al. suggested that the surface aggregation might be driven by the compression of Langmuir monolayers, in the form of a surface concentration dependent on the critical micelle concentration.[32] Lennox et al. thought that the spreading solvent acted as a medium for the block polymer to find a quasi-equilibrium conformation and the formation of surface aggregates was a spontaneous surface aggregation process that was neither compression-induced, associated with micellization in the spreading solution, nor induced by the LB film transfer process.[33] In our case, EO_7OPV is monodisperse in chloroform, confirmed by the UV−vis spectrum (curve b in Figure 3, the maximal absorption peak at 367 nm corresponding to the OPV monomer). The aggregates of EO_7OPV are formed even at the surface pressure of 0 mN/m. In addition, the formation of surface aggregates is independent of the spreading solution concentration. The surface aggregation of EO_7OPV is driven by the hydrophobic interaction between the OPV block and the PEO block or water and by the strong $\pi-\pi$ stacking interaction between EO_7OPV molecules. Surprisingly, the sizes of some EO_7OPV domains deposited at 1 and 2 mN/m are much larger than those at the higher surface pressures. From the magnified Figure 2A and 2B, we can see that the irregular-shaped islands have some cracks and comprise some smaller domains. The various sizes of the irregular-shaped domains may mean that the coalescence of those small aggregates occurs during the transfer process of EO_7OPV monolayers. According to the $\pi-A$ isotherm for EO_7OPV, the Langmuir monolayer of EO_7OPV below the surface pressure of 3 mN/m (at the molecular area of 60−40 Å^2) is unstable due to the molecular rearrangement (vide supra), which leads to the low transfer ratios of LB monolayers. Interestingly, the shape and size of domains are nearly unchangeable in the range of surface pressures from 3 to 12 mN/m, and only the space between domains becomes closer. We, therefore, believe that these aggregate domains are stable in the range of surface pressures from 3 to 12 mN/m. The critical surface pressure forming stable aggregate domains is proposed to be 3 mN/m, corresponding to a molecular area of 40 Å^2 (close to the limiting area).

Figure 2G shows the cross-sectional analysis of the LB monolayer at the surface pressure of 4 mN/m. The surface of domains is homogeneous and the height of domains is about 3.6 nm. The similar domain heights were observed at other surface pressures, low and high pressures. Combining the OPV rod length of 1.85 nm calculated from Cerius^2 molecule dynamic simulation and the fiber-axis length of 1.948 nm in the crystal structure of the PEO coil,[29] the monomolecular length of EO_7-OPV should be 3.8 nm, which is in agreement with the thickness of the EO_7OPV domain in the LB monolayer determined by the AFM measurements. Additionally, the UV−vis absorption spectrum of the transferred monolayer at the surface pressure of 12 mN/m presents the maximal absorption peak at 302 nm (curve a in Figure 3). Compared with the absorption peak of the OPV monomer at 367 nm (curve b in Figure 3), the large blue-shift of 65 nm in the LB monolayers of EO_7OPV indicates that the H-aggregate is formed due to the strong $\pi-\pi$ stacking interaction between the OPV blocks.[34] Therefore, a structural model is proposed in Figure 2H, where the flexible and hydrophilic PEO blocks are adsorbed onto the mica substrate, while the rigid and hydrophobic OPV blocks form an ordered crystalline OPV layer through the $\pi-\pi$ stacking interaction.

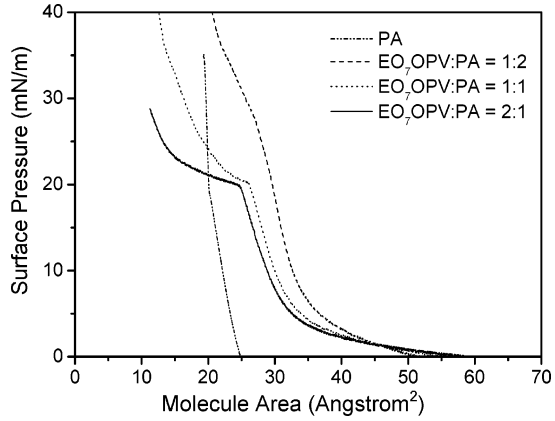

Figure 4. The pressure−area ($\pi-A$) isotherms for the PA monolayer and the mixed monolayers of EO_7OPV and PA at the molar ratio of 2:1, 1:1, and 1:2.

Similar observations have also been found in the casting films of this kind of rod−coil diblock molecules.[25,26]

Length-Controlled Rodlike Domains of EO_7OPV in Binary Mixed LB Monolayers. Figure 4 shows the $\pi-A$ isotherms for PA and the EO_7OPV/PA mixtures at the molar ratio of 2:1, 1:1, and 1:2. The phase transition from liquid-expanded (LE) to liquid-condensed (LC) state in the PA monolayer is continuous, with a small decrease in headgroup area, around 19 mN/m and 20 Å^2/molecule, which is consistent with the earlier report.[35] Since the surface pressure of the phase transition of PA is close to the collapse pressure of mixed Langmuir films, the phase transition of PA in the $\pi-A$ isotherms of mixed Langmuir films is not observed. For the ideally miscible or completely phase-separated mixed monolayers, there exists a proportional rule between the mixed ratio and the average molecular area at a certain surface pressure.[36] The mixed monolayers of EO_7OPV and PA do not show the proportional regularity. However, in the following text, the morphological studies of mixed LB monolayers of EO_7OPV and PA indicate that EO_7OPV and PA are phase-separated in the mixed Langmuir monolayers. The unproportionate regularity of $\pi-A$ isotherms for EO_7OPV/PA mixed monolayers may be attributed to the change of the average density and molecular orientations according to the mixing ratio.

The AFM technique provides direct information of heterogeneous domains as well as nanoscale structure and surface properties of heterogeneous multicomponent monolayers. Herein, we used the AFM technique to examine the morphology of the mixed LB monolayers of EO_7OPV and PA. Figure 5 shows the AFM height images of the LB monolayers of EO_7OPV and PA deposited onto the mica substrates at a molar ratio of 2:1, 1:1, and 1:2 at surface pressures of 6 mN/m and 12 mN/m. In all samples, we observed some brighter rodlike domains and darker islands. The terminals of the rodlike domains are mostly conjoint. The rodlike domains seem to have several special directions. The angles of two directions for the rods are mostly about 60° and 120°. The height difference between the brighter rodlike domains and the darker islands is about 1.6 ± 0.3 nm, which is consistent with the expected difference between monolayers of EO_7OPV (3.6 nm) and PA (2.0 nm). Furthermore, at the same surface pressure, the coverage area of rodlike domains decreases with the increase of the molar fraction of PA. The decrease of coverage area of rodlike domains with the increase of the molar fraction of PA and the height difference between the brighter rodlike domains and the darker islands indicate that the brighter rodlike domains consist of EO_7OPV and the darker islands are the close-packed monolayer of PA. The cross section of the AFM height image of the EO_7OPV/PA mixed monolayer at a molar ratio of 1:2 at the surface pressure of 6 mN/m is shown in Figure 6. The average thickness of the darker islands of PA is 0.6 nm and that of the brighter rodlike domains of EO_7OPV is 2.4 nm. Since the monolayer height of PA is 2.0 nm and that of EO_7OPV is 3.6 nm, the space among rodlike domains and darker islands should be another phase. According to the earlier report,[37] the Langmuir monolayer of PA was the LE phase and LC phase coexistence in the range of the molecular areas from 40 to 20 Å^2. The AFM images of the monolayer of PA deposited onto mica in this range presented the close-packed LC phase coexisting with the less-ordered LE phase, and the height difference of these two phases was 0.5−0.8 nm. On the basis of the $\pi-A$ isotherms for mixed monolayers of EO_7OPV and PA (Figure 4), there is the two-phase coexistence of PA at surface pressures of 6 and 12 mN/m. The height difference of 0.6 nm between the darker island and the space among brighter rodlike domains and darker islands is in good agreement with the height difference between the close-packed LC phase and the less-ordered LE phase of PA. Hence, we suggest that the darker islands are the close-packed LC phase of PA and the space among rodlike domains and darker islands is the less-ordered LE phase of PA.

At a certain molar ratio of EO_7OPV/PA, the rodlike domains consisting of EO_7OPV are very uniform in size and shape in the range of surface pressures from 3 to 12mN/m. However, the domains consisting of EO_7OPV in mixed LB monolayers do not present regular shapes and uniform sizes when transferred below the surface pressure of 3 mN/m. These results are similar to those of pure EO_7OPV (Figure 2). The rodlike domains in mixed LB monolayers are elongated compared with the domains in LB monolayers of pure EO_7OPV. The widths of the rods formed at different mixed ratios are similar, which are about 290 ± 40 nm. Interestingly, the length of the rods increases prominently with the increase of the molar ratio of PA. The average length is about 1.0 μm at a molar ratio of 2:1, 1.5 μm at a molar ratio of 1:1, and 3.2 μm at a molar ratio of 1:2. We further investigated the morphology of the mixed LB monolayers at other molar ratios. When the molar ratio of EO_7OPV/PA was 5:1, the shorter rodlike domains (0.76 μm) with regular shape could be obtained. When the molar ratio of EO_7OPV/PA was modified to be 1:5, the longest rods of about 13.8 μm were formed at the surface of 6 mN/m; however, many irregular domains consisting of EO_7OPV were also observed. The relationship between the average length of the rodlike domains and the molar ratio of EO_7OPV/PA is summarized in Table 1. On the basis of these experimental results, we consider that the mixed ratio of EO_7OPV and PA should be responsible for the presence of the rodlike domains with well-defined shapes and sizes. We suggest that when the EO_7OPV/PA molar ratio is larger than 1:2, it is more advantageous to form well-defined rods. The length of rodlike domains may be tuned roughly from 0.3 to 13.8 μm by altering the molar ratio of EO_7OPV and PA.

Domain Shape. In view of the above results, a series of regular-shaped rodlike domains consisting of EO_7OPV have been obtained through utilizing the phase separation of EO_7-OPV and PA at the air−water interface. It is very important to note that the length of rodlike domains increases with the increase of the molar fraction of PA. The elongation degree of the rods is systematically consistent with the content of PA. Furthermore, at a certain molar ratio of EO_7OPV/PA, the shape and size of the rods do not change in the range of surface pressures from 3 to 12 mN/m. Therefore, we believe that the

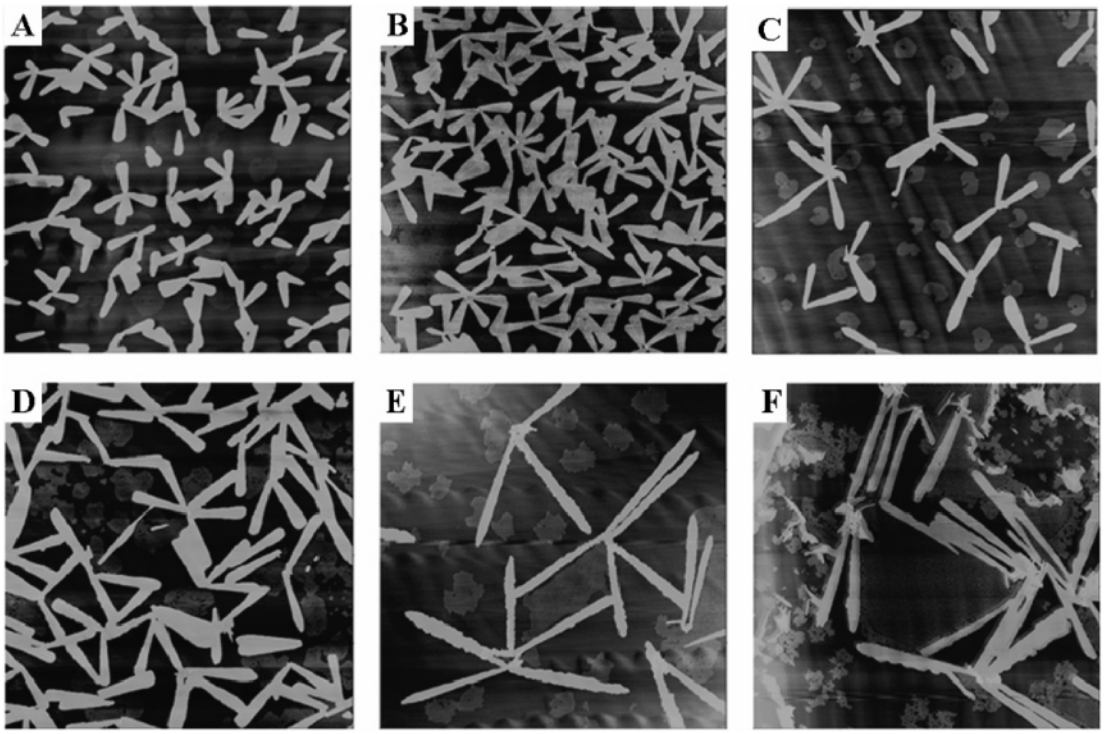

Figure 5. AFM height images (10 × 10 μm) of the mixed monolayers of EO_7OPV and PA transferred onto mica at different EO_7OPV/PA molar ratios and at different surface pressures: (A) 2:1 at 6 mN/m, (B) 2:1 at 12 mN/m, (C) 1:1 at 6 mN/m, (D) 1:1 at 12 mN/m, (E) 1:2 at 6 mN/m, and (F) 1:2 at 12 mN/m, respectively. *Z* range, 20 nm.

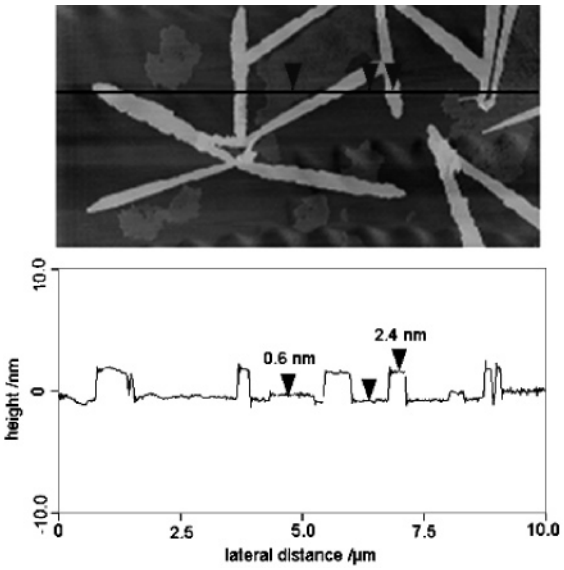

Figure 6. A cross-sectional analysis for the AFM height image of the transferred monolayer of EO_7OPV and PA at a molar ratio of 1:2 at the surface pressure of 6 mN/m.

TABLE 1: Average Length of Rodlike Domains of EO_7OPV with Respect to the Molar Ratio of EO_7OPV/PA

average length of rodlike domains (μm)	0.35	0.76	1.0	1.5	3.2	13.8[a]
molar ratio of EO_7OPV/PA	1/0	5/1	2/1	1/1	1/2	1/5

[a] The length of rods is uneven and 13.8 μm is the largest length of rods at the surface pressure of 6 mN/m.

rodlike domains on mica do not form during the transfer process, but form at the air−water interface.

At the air−water interface, there are several cases causing the elongated domains. Kato et al. reported the formation of elongated domains in the binary mixed Langmuir monolayer and observed that the elongated domains could be transformed to circular ones at a higher temperature.[17] They believed that the elongated domains were a quenched structure after complete solvent evaporation, because the molecular motion was extremely suppressed at the lower temperature. In our case, we find that the elongated shape and size of EO_7OPV domains are similar at different interface temperatures (5, 20, and 32 °C), which indicates that the rodlike domains of EO_7OPV in mixed monolayer are less likely quenched structures. In addition, the rodlike domains have regular shape and smooth boundaries. Therefore, we consider that the rodlike domains of EO_7OPV are in equilibrium at the air−water interface. The equilibrium shape of domains at the air−water interface should be controlled by the line tension of interface between the two phases and by the long-range electric dipolar interactions between molecules.[22,23] The increase of the line tension between two phases is beneficial to the formation of circular domains, while the increase of the long-range electric dipolar interactions between molecules is advantageous to the elongation shape of domains. For example, Sparr et al. have reported that the addition of cholesterol, a line tension lowering material, led to the domain elongation of ceramides *N*-hexadecanoyl-phytosphingosine (C_{16}-CerIII) or *N*-tetracosanoyl-phytosphingosine (C_{24}CerIII) due to the decrease of the line tension.[38] However, in the mixed monolayer of EO_7OPV and PA, PA is a line tension increasing material due to its long alkyl chain and small headgroup. Although the rodlike domains consisting of EO_7OPV are gradually elongated with the increase of the molar fraction of PA, the elongation origin of the rods should be different from that reported by Sparr. The long-range electric dipolar interactions between molecules may play a key role in the equilibrium shape of domains in some systems.[19,20] Gallet et al. reported that the introduction of horizontal dipole interaction between molecules could lead to the needlelike domains in nitrobenzoxadiazole (NBD)−stearic acid films.[20] McConnell et al. reported that the chiral and spiral solid domains in monolayers

of lipid molecules resulted from the long-range molecular orientational order of the hydrocarbon chain.[19] In fact, these long-range electric dipolar interactions between molecules are believed to be an anisotropic interaction, which should be an essential factor leading to the domain elongation. In our case, due to the strong $\pi-\pi$ stacking interaction between the OPV blocks, the rodlike domains consisting of EO_7OPV form H-aggregates in which the molecules are tilted with respect to the plane of the monolayer. The $\pi-\pi$ stacking interaction between the OPV blocks is a long-range electric dipolar interaction parallel to the plane of the monolayer. EO_7OPV can aggregate along the $\pi-\pi$ stacking direction at the air−water interface. Hence, we suggest that, driven by the $\pi-\pi$ stacking interaction, the long-range molecular orientational order of the OPV blocks leads to the elongated shape of EO_7OPV domains.

Then, why are the rods prominently elongated with the increase of the molar fraction of PA? That should be concerned with the formation mechanism of the phase-separated rodlike domains. The nucleation and growth (NG) mechanism, similar to the crystal formation mechanism, may be used to demonstrate the phase-separated domain formation in mixed LB films.[17] In our presented case, the NG mechanism is plausible for the formation of elongated domains of EO_7OPV. When the mixed solution of EO_7OPV and PA was spread at the air−water interface, EO_7OPV first aggregated and formed anisotropic nuclei with the long-range molecular orientational order of the OPV blocks, driven by the $\pi-\pi$ stacking interaction between the OPV blocks. The EO_7OPV molecules should be very mobile at the air−water interface, and thus EO_7OPV molecules near the anisotropic nucleus were transported toward the nucleus and converted to a condensed phase along the $\pi-\pi$ stacking direction of the nucleus, while PA molecules were excluded from the condensed phase of EO_7OPV. Finally EO_7OPV formed rodlike domains and presented elongated shapes. For the NG mechanism, the growth of domains was related to the nucleus number. Fewer nuclei would be more advantageous to the domain growth. In our mixed Langmuir monolayers, the nucleus number of EO_7OPV should decrease with the increase of the molar fraction of PA, which should make it possible for the domains of EO_7OPV to grow larger. Therefore, EO_7OPV might grow into large and elongated domains with the increase of the molar fraction of PA.

Oriented Rodlike Domains on Mica. Interestingly, the rodlike domains consisting of EO_7OPV seem to have several special directions (Figure 5). The angles of two directions for the rodlike domains are mostly about 60° or 120°. The special directions of the domains in LB monolayers of pure EO_7OPV are also observed, though they are not obvious (Figure 2E). The similar-oriented arrangement of self-assembled domains on mica has also been found in other systems.[39−42] Akutagawa et al. reported that an amphiphilic bis-tetrathiafulvalene substituted macrocycle could form nanowires at the air−water interface and the nanowires transferred from a dilute aqueous metal choride subphase could self-assemble along the directions of the metal ion array on the mica surface having 6-fold symmetry during the film deposition process.[42] They believed that the oriented self-assembled domains deposited onto mica resulted from the template inducement of metal ion array on the crystalline mica surface having 6-fold symmetry. In our case, the PEO block with 7 repeating units may be similar to 18-crown-6, interacting with K^+ cations. Hence, rodlike domains consisting of EO_7OPV may recognize the K^+ cation array on the mica surface having 6-fold symmetry during the film deposition process, and present an oriented arrangement on mica. We think, similar to that reported by Akutagawa and co-workers, that the formation of the oriented rodlike domains on mica is governed by two processes: aggregation of EO_7OPV molecules into the elongated rodlike domains at the air−water interface and self-assembly of rodlike domains along the directions of the K^+ array on the mica surface having 6-fold symmetry during the film deposition process.

We suggest that the existence of the LE phase of PA in mixed Langmuir monolayers makes rodlike domains easy to orient on the crystalline mica surface during the film deposition process. At lower surface pressures, the rodlike domains of EO_7OPV should be surrounded by the more LE phase and less LC phase of PA, which is more advantageous to the oriented self-assembly of rodlike domains on the crystalline mica surface. Hence, the orientations of the rodlike domains should be more obvious at 6 mN/m than at 12 mN/m, which is in agreement with the experimental results (Figure 5). Additionally, we observed the AFM images of mixed LB monolayers of EO_7OPV and PA deposited onto the amorphous silica substrate at the surface pressure of 6 mN/m. The rodlike domains are formed, but the alignment of rods is disordered, which indicates that the oriented arrangement of the rodlike domains on mica may be induced by the crystalline surface of mica.

Conclusion

In summary, regular-shaped and regular-sized rods consisting of EO_7OPV are fabricated on mica through utilizing the phase separation of EO_7OPV and PA by the LB technique. A series of rodlike domains consisting of EO_7OPV with different lengths can easily be obtained by changing the molar ratio of EO_7OPV and PA. The length of rods may be tuned in a large range. In addition, the rodlike domains may self-assemble along the directions of the 6-fold symmetric array of K^+ cation on the mica surface during the transfer process. We demonstrate the possible formation mechanism of rodlike domains in mixed LB monolayers and propose the two-step formation process of oriented rodlike domains deposited onto the mica substrates. Because the molecules containing the OPV and PEO block are one of promising electrooptical materials,[43,44] these nanostructures of EO_7OPV domains may be applied potentially in diversiform molecular devices. Although further optimization of the molecular design and electrooptical property will be needed, the principle to control the length and oriented arrangement of self-assemblies by the LB technique will be quite significant to molecular electronic devices.

Acknowledgment. This work was supported by financial support from the National Natural Science Foundation of China (Grant No. 29992590-5), the Major State Basic Research Development Program (Grant No. G2000078102), and the Ministry of Education of China. Our research is also supported by the State Key Laboratory of Polymer Physics and Chemistry.

References and Notes

(1) Lehn, J.-M. *Supramolecular Chemistry*; VCH: New York, 1995.
(2) Whitesides, G. M. *Sci. Am.* **1995**, 146.
(3) Stupp, S. I.; LeBonheur, V.; Walker, K.; Li, L. S.; Huggins, K. E.; Keser, M.; Amstutz, A. *Science* **1997**, *276*, 384.
(4) Zhang, X.; Shen, J. C. *Adv. Mater.* **1999**, *11*, 1139.
(5) Jenekhe, S. A.; Chen, X. L. *Science* **1999**, *283*, 372.
(6) Lee, M.; Cho, B.-K.; Zin, W.-C. *Chem. Rev.* **2001**, *101*, 3869.
(7) Klok, H.-A.; Lecommandoux, S. *Adv. Mater.* **2001**, *13*, 1217.
(8) Tsukruk, V. V.; Genson, K.; Peleshanko, S.; Markustsya, S.; Lee, M.; Yoo, Y.-S. *Langmuir* **2003**, *19*, 495.
(9) Cho, B.-K.; Lee, M. *J. Am. Chem. Soc.* **2001**, *123*, 9677.
(10) Chen, J. T.; Thomas, E. L.; Ober, C. K.; Mao, G.-P. *Science* **1996**, *273*, 343.

(11) Overney, R. M.; Meyer, E.; Frommer, J.; Brodbeck, D.; Luthi, R.; Howald, L.; Gunterodt, H.-J.; Fujihira, M.; Takano, H.; Gotoh, Y. *Nature (London)* **1992**, *359*, 133.
(12) Duschl, C.; Liley, M.; Vogel, H. *Angew. Chem., Int. Ed. Engl.* **1994**, *33*, 1274.
(13) Jacobi, S.; Chi, L. F.; Funchs, H. *J. Vac. Sci. Technol. B* **1996**, *14*, 1503.
(14) Gamboa, A. L. S.; Filipe, E. J. M.; Brogueira, P. *Nano Lett.* **2002**, *2*, 1083.
(15) Ekelund, K.; Sparr, E.; Engblom, J.; Wennerström, H.; Engström, S. *Langmuir* **1999**, *15*, 6946.
(16) Moraille, P.; Badia, A. *Langmuir* **2002**, *18*, 4414.
(17) Iimura, K.-I.; Shiraku, T.; Kato, T. *Langmuir* **2002**, *18*, 10183.
(18) Weis, R. M.; McConnell, H. M. *J. Phys. Chem.* **1985**, *89*, 4453.
(19) Moy, V. T.; Keller, D. J.; Gaub, H. E.; McConnell, H. M. *J. Phys. Chem.* **1986**, *90*, 3198.
(20) Muller, P.; Gallet, F. *J. Phys. Chem.* **1991**, *95*, 3257.
(21) Knobler, C. M. *Science* **1990**, *249*, 870.
(22) McConnell, H. M.; Moy, V. T. *J. Phys. Chem.* **1988**, *92*, 4520.
(23) McConnell, H. M.; DeKoler, R. J. *J. Phys. Chem.* **1992**, *96*, 7101.
(24) Xiong, H. M.; Qin, L. D.; Sun, J. Q.; Zhang, X.; Shen, J. C. *Chem. Lett.* **2000**, 586.
(25) Qin, L. D.; Wu, L. X.; Li, H. B.; Hou, X. L.; Qiu, D. L.; Shen, J. C. *Chem. Lett.* **2002**, 720.
(26) Qin, L. D.; Li, H. B.; Wu, L. X.; Qiu, D. L.; Zhang, X.; Shen, J. C. *Chem. Lett.* **2003**, *32*, 390.
(27) Kuzmenka, D. J.; Granick, S. *Macromolecules* **1988**, *21*, 779.
(28) Tew, G. N.; Pralle, M. U.; Stupp, S. I. *J. Am. Chem. Soc.* **1999**, *121*, 9852.
(29) Takahashi, Y.; Tadokoro, H. *Macromolecules* **1973**, *6*, 672.
(30) Bijsterbosch, H. D.; de Haan, V. O.; de Graaf, A. W.; Mellma, M.; Leermakers, F. A. M.; Cohen Stuart, M. A.; van Well, A. A. *Langmuir* **1995**, *11*, 4467.
(31) Goncalves da Silva, A. M.; Simoes Gamboa, A. L.; Martinho, J. M. G. *Langmuir* **1998**, *14*, 5327.
(32) An, S. W.; Su, T. J.; Thomas, R. K.; Baines, F. L.; Billingham, N. C.; Armes, S. P.; Penfold, J. *J. Phys. Chem. B* **1998**, *102*, 387.
(33) Cox, J. K.; Yu, K.; Constantine, B.; Eisengberg, A.; Lennox, R. B. *Langmuir* **1999**, *15*, 7714.
(34) Watakabe, A.; Okada, H.; Kunitake, T. *Langmuir* **1994**, *10*, 2722.
(35) Bibo, A. M.; Peterson, I. R. *Adv. Mater.* **1990**, *2*, 309.
(36) Gains, L. G. *Insoluble Monolayers at Liquid−Gas Interfaces*; Interscience Publishers: New York, 1990.
(37) Vickery, S. A.; Dunn, R. C. *Langmuir* **2001**, *17*, 8204.
(38) Sparr, E.; Eriksson, L.; Bouwstra, J. A.; Ekelund, K. *Langmuir* **2001**, *17*, 164.
(39) Samorí, P.; Francke, V.; Müllen, K.; Rabe, J. P. *Thin Solid Films* **1998**, *336*, 13.
(40) Samorí, P.; Francke, V.; Müllen, K.; Rabe, J. P. *Chem.—Eur. J.* **1999**, *5*, 2312.
(41) Xu, J.; Zhou, C.-Z.; Yang, L. H.; Chung, N. T. S. Chen, Z.-K. *Langmuir* **2004,** *20*, 950.
(42) Akutagawa, T.; Ohta, T.; Hasegawa, T.; Nakamura, T.; Chistensen, C. A.; Becher, J. *Proc. Natl. Acad. Sci. U.S.A.* **2002**, *99*, 5028.
(43) Benfaremo, N.; Sandman, D. J.; Tripathy, S.; Kumar, J.; Yang, K.; Rubner, M. F.; Layons, C. *Macromolecules* **1998**, *31*, 3595.
(44) Tao, Y.; Donat-Bouillud, A.; D'Iorio, M.; Lam, J.; Gorjanc, T. C.; Py, C.; Wong, M. S.; Li, Z. H. *Thin Solid Films* **2002**, *363*, 298.